

Multifrequency Behaviour of the Gamma-Ray Binary System PSR B1259-63: Modelling the FERMI Flare

Brian van Soelen¹, Pieter J. Meintjes¹

¹*Department of Physics, University of the Free State, Bloemfontein 9300, South Africa*

Corresponding author: vansoelenb@ufs.ac.za

Abstract

This paper presents a brief overview of the multifrequency properties of the gamma-ray binary system PSR B1259-63 from radio to very high energy gamma-rays. A summary is also presented of the various models put forward to explain the Fermi “flare” detected in 2011. Initial results are presented of a new turbulence driven model to explain the GeV observations.

Keywords: Gamma-ray binaries - individual: PSR B1259-63.

1 Introduction

There are only a handful of known gamma-ray binary systems. Of these, it is only in PSR B1259-63 that the nature of the compact object is known due to the detection of pulsed radio emission (Johnston et al., 1992a). The Very High Energy (VHE) nature of the source was confirmed by the H.E.S.S. telescope around the 2004 periastron passage (Aharonian et al., 2005). The gamma-ray binary system consists of a 48 ms pulsar, in an eccentric ($e = 0.87$) 3.4 year orbit around a Be star (e.g. Johnston et al., 1992, 1994), with a spin-down luminosity of $\dot{E} = 8.3 \times 10^{35}$ erg s⁻¹ (e.g. Wang et al., 2004). Recent spectroscopic observations have placed better constraints on the parameters of the optical companion, LS 2883, and the binary system (Negueruela et al., 2011).

In this paper, we present an overview of the multifrequency behaviour of PSR B1259-63, and discuss some of the modelling undertaken to explain the large “flare” event detected by Fermi after the previous periastron passage.

2 Multifrequency Observations

In this section we summarize the multifrequency behaviour of the non-thermal emission originating from PSR B1259-63, discussing the radio, X-ray, VHE gamma-ray and, finally, the GeV gamma-ray observations.

2.1 Radio behaviour

PSR B1259-63 was originally detected as a radio pulsar during a galactic plane survey undertaken with the

64 m Parkes radio telescope (Johnston et al., 1992b). Observations around periastron showed that there was an increase (and variability) in the dispersion measurement of the pulsed signal and an eclipse of the pulsed signal between approximately 20 days before periastron to 20 days after (e.g. Johnston et al., 1996, 1999, 2001). Significantly, around periastron an unpulsed and variable radio emission was detected with a flux density of 10 – 30 mJy, higher than the flux of the pulsed signal (2 – 3 mJy). These observations are explained by the pulsar passing through and/or behind the circumstellar disc of the Be star, and the formation of synchrotron emission in the pulsar wind nebula. More recently a large extended pulsar wind nebula has also been reported around periastron by Moldón et al., (2011).

2.2 X-ray behaviour

A non-thermal X-ray component has been detected from PSR B1259-63 across the whole of the orbit, with early detections determining a luminosity of $L \sim 10^{34}$ erg s⁻¹ around periastron (Kaspi et al., 1995). Combined *ASCA*, *Chandra*, *XMM-Newton*, *BeppoSAX*, *Swift* and *Suzaku* observations covering the 1997 – 2010 periastron passages have shown a consistent X-ray light curve (see Chernyakova et al., 2006, 2009, Abdo et al., 2011, and references therein). These datasets have presented particular coverage focused on the disc crossing epochs. The observations show that the X-ray emission peaks within two narrow time bands most likely associated with the pulsar approaching the circumstellar disc. Pavlov et al., (2011) also reported on an extended X-ray structure detected by *Chandra* near apastron. The observations in the 0.5–8 keV en-

ergy band showed an elongated structure ($\sim 4''$) with a luminosity of $\sim 10^{32}$ erg s $^{-1}$ (assuming a distance of 3 kpc). It is likely that this is associated with the pulsar wind nebula outflow.

2.3 VHE behaviour

PSR B1259-63 was detected for the first time at VHE with the H.E.S.S. telescope during the 2004 periastron passage (Aharonian et al., 2005). The observations showed a variable light curve with an implied maximum flux a few days before and after periastron. The system has since been detected during 2007 (Aharonian et al., 2009) and 2011 (Abramowski et al., 2013), albeit with much less coverage. The H.E.S.S. observations appear to be consistent with the double peak structure observed at X-ray and radio wavelengths, but this conclusion is not definitive due to lower coverage during the pre-periastron approach of the pulsar. The spectrum of the VHE emission also appears to be consistent with a single power-law distribution, with no cut-off in the spectrum (see e.g. fig. 4 in Abramowski et al., 2013).

While the coverage over the last periastron passage was poor, the 2011 observations were coincident with the Fermi “flare” discussed in the next section. Unlike the Fermi detection, the H.E.S.S. observations showed no significant change between the pre- and post-flare event, and morphologically the GeV to TeV energies are not consistent with a single power-law distribution (see fig. 5 in Abramowski et al., 2013).

2.4 HE behaviour

Due to the consistency of the radio, X-ray and VHE light curves, it was presumed (before 2010/2011) that Fermi would observe similar behaviour. In fact, it was not actually clear whether the system would be detectable by Fermi (e.g. Chernyakova et al., 2009). The gamma-ray detection and rapid transient behaviour that were reported by Fermi were completely unexpected.

As reported by Abdo et al. (2011), the system was relatively undetected before periastron, with a faint “brightening” phase which began around the point of the first disc crossing and lasted until ~ 18 days after periastron. However, approximately 30 days after periastron, there was a rapid increase in the detected emission from the source showing an average flux of $F(> 100\text{MeV}) = (4.4 \pm 0.3_{\text{stat}} \pm 0.7_{\text{sys}}) \times 10^{-10}$ erg cm $^{-2}$ s $^{-1}$, with a photon index of $\Gamma = (1.4 \pm 0.6_{\text{stat}} \pm 0.2_{\text{sys}})$ and a cutoff energy $E_c = (0.3 \pm 0.1_{\text{stat}} \pm 0.1_{\text{sys}})$ GeV. This “flare” was detected until > 60 days after periastron. Significantly, radio, X-ray, and VHE observations showed no unusual or flaring events. Most surprisingly, the daily binned light curve showed a peak luminosity of

$L_\gamma \approx 8 \times 10^{35}$ erg s $^{-1}$ (for isotropic emission at an assumed distance of 2.3 kpc), corresponding to ≈ 100 per cent of the spin-down power of the pulsar.

The emission detected by Fermi has proved difficult to reconcile with models of the system. In the next section we discuss some of the models pertaining to GeV energies and the Fermi flare.

3 Modelling the Fermi Flare

3.1 Effect of the infrared excess

In anticipation of the Fermi observations of PSR B1259-63, van Soelen & Meintjes (2011), van Soelen et al. (2012) and Meintjes & van Soelen (2012), considered the influence the infrared flux from the circumstellar disc of the Be star would have on gamma-ray production. If the same population of electrons which produces the VHE emission through inverse Compton scattering of the optical photons, scatters the infrared photons from the disc, it will produce emission in the GeV energy range. First using an isotropic approximation (van Soelen & Meintjes, 2011) and then a full anisotropic approximation, which took into account the anisotropic inverse Compton scattering as well as the changing flux from the circumstellar disc as measured from the pulsar’s position (van Soelen et al., 2012), we showed that the scattering of the infrared photons would increase the flux at GeV energies by a factor of 2. While it was thought that the large size of the circumstellar disc would result in it dominating near the disc crossing, we found that the low density of the disc mitigated this effect as the majority of the infrared emission occurred near the star and not far out in the disc. However, the flux was below what was detected by Fermi.

3.2 Cold pulsar wind

Khangulyan et al. (2012) proposed that the scattering of the cold pulsar wind ($\gamma = 10^4$) off photons from the circumstellar disc, after the second disc passage, could produce the observed Fermi flare. The authors propose that the shock-front around the pulsar is confined within the disc, and after the pulsar leaves the circumstellar disc the opening of the shock structure will allow the inverse Compton scattering of the cold pulsar wind to produce the flare. One problem presented by this model is the number of additional photons required to do this. The authors estimate that the additional photon distribution must have a luminosity of approximately 40 per cent of the stellar luminosity. This does not appear to be consistent with the observations obtained around periastron nor with the estimation of the available energy from shock-heating (van Soelen et al., 2012). However, it must be cautioned that the reported observations were not undertaken at the same time as

the Fermi flare and new observations around the next periastron passage must be obtained, to obtain better constraints.

3.3 SPH modelling

A process of smooth particle hydrodynamic (SPH) modelling of PSR B1259-63 was undertaken by Takata et al., (2012) to model the behaviour of the Be star's circumstellar disc around periastron. The simulations show that the disc should be considerably disrupted during the pulsar crossing. However, observations on 5 January 2011, approximately three weeks after periastron, showed that the mid-infrared flux was consistent with previous observations (see van Soelen et al., 2012). This suggests that either the disc was not dramatically effected, or that there was a rapid recovery.

In addition, the approximation of the emission light curve, while in agreement with the X-ray emission, was not in agreement with the GeV light curve, as the simulations suggested that the maximum emission should occur before periastron (see figs. 3 and 5 in Takata et al., 2012).

3.4 Doppler boosting emission

The most recent model which has been suggested is that the synchrotron emission is Doppler boosting to GeV energies to produce the observed flare. This was modelled in detail by Kong et al. (2012). The authors consider two emission regions along the shock front: the first near the apex with a bulk Lorentz factor of $\Gamma = 1$ and the second along the shock tail which is mildly relativistic ($\Gamma_{\max} \approx 2$) and is beamed along the shock.

These simulations are able to account for the Fermi detection during the flare period, but are not so successful during the pre-periastron period – though it should be noted that the pre-periastron detections have a much lower significance. The light curve predictions also suggest only a single peaked emission around periastron for the GeV energies, and a double peaked structure from the X-ray and VHE emission. However, the modelled light curves predict a higher flux for the GeV and TeV emission around periastron (see fig. 5 in Kong et al., 2012), an effect which is not observed.

3.5 Turbulence driven emission?

Thus far all models have presented unique problems in modelling the Fermi flare. For this reason it is still necessary to consider alternative models. Below we consider the possibility of a turbulence induced flare.

Hydrodynamical simulations of colliding wind systems have shown that Kelvin-Helmoltz instabilities develop along the dividing line between the pulsar and stellar winds (see e.g. Bosch-Ramon et al., 2012). If

these instabilities form a turbulent medium, it may be possible for secondary particle acceleration to occur due to second-order Fermi acceleration (see e.g. Bosch-Ramon & Rieger 2012). It has been considered by a number of authors that under the effect of radiative cooling and second-order Fermi acceleration, a Maxwellian-like distribution will form (see e.g. Schlickeiser 1985 for a discussion of first- and second-order acceleration with radiative cooling). Such a secondary distribution of electrons may be responsible for producing the GeV emission in PSR B1259-63 if acceleration in the turbulent region occurs around the second disc crossing.

As a first approximation we consider the modified Maxwellian distribution suggested by Stawarz & Petrosian (2008), given by

$$n_e = n_0 \gamma^2 \exp \left[-\frac{1}{a} \left(\frac{\gamma}{\gamma_{\text{eq}}} \right)^a \right], \quad (1)$$

where $a = 3 - q$ for dominant synchrotron/Thomson-limit inverse Compton cooling, or $a = 1.5 - q$ for dominant Klein-Nishina inverse Compton cooling. Here q is the index of the turbulence power-law, and γ_{eq} is determined by equating the appropriate radiative cooling time to the acceleration time (see Stawarz & Petrosian, 2008, and reference therein, for details related to the acceleration).

We calculate the best fit inverse Compton emission for the electron distribution given by equation (1) for isotropic scattering (e.g. Blumenthal & Gould, 1970), with a blackbody distribution of photons ($T_* = 33\,000$ K). In this first approximation an isotropic radiation field has been assumed.

The equilibrium energies required to fit the Maxwellian distributions (equation 1) were found to be $\gamma_{\text{eq}} = 1614.4$ for the Bohr approximation ($q = 1$), $\gamma_{\text{eq}} = 656.30$ for the hard-sphere approximation ($q = 2$), $\gamma_{\text{eq}} = 1030.4$ for the Kolmogorov spectrum ($q = 5/3$) and $\gamma_{\text{eq}} = 1196.7$ for the Kraichnan spectrum ($q = 3/2$). Only $a = 3 - q$ was considered. A constant factor was applied to match the flux level of the flare. The resulting fits are shown in Fig. 1.

The figure shows that the distribution produces a reasonable fit to the resulting Fermi detection. Initial considerations of the parameter space suggest that it may be possible to accelerated electrons to the appropriate energies around the period of periastron. A more detailed analysis is currently under-way.

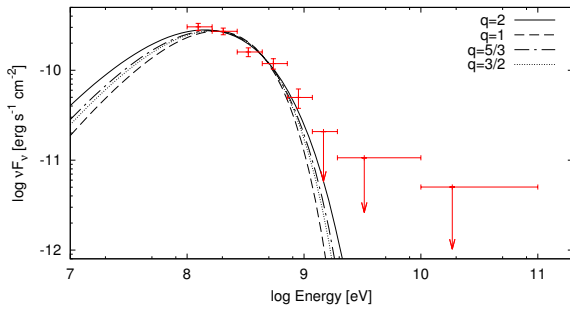


Figure 1: Inverse Compton spectrum formed by a modified Maxwellian electron distribution fitted to the post-periastron Fermi flare detection.

References

- [1] Abdo, A.A., Ackermann, M., Ajello, M. et al.: 2011, *ApJ*, 736, L11 [doi:10.1088/2041-8205/736/1/L11](https://doi.org/10.1088/2041-8205/736/1/L11)
- [2] Aharonian, F., et al. (H.E.S.S. Collaboration): 2005, *A&A*, 442, 1
- [3] Aharonian, F., et al. (H.E.S.S. Collaboration): 2009, *A&A*, 507, 389
- [4] Abramowski, A., et al. (H.E.S.S. Collaboration): 2013, *A&A*, 551, A94
- [5] Blumenthal, G.R., Gould, R.J.: 1970, *Reviews of Modern Physics*, 42, 237
- [6] Bosch-Ramon, V., Rieger F.M.: 2012, in *Astroparticle, Particle, Space Physics and Detectors For Physics Applications - Proceedings of the 13th ICATPP Conference..* G. Simone et al. (eds.), 219
- [7] Bosch-Ramon, V., Barkov, M.V., Khangulyan, D., et al.: 2012, *A&A*, 544, 59
- [8] Chernyakova, M., Neronov A., Lutovinov A., et al.: 2006, *MNRAS*, 367, 1201 [doi:10.1111/j.1365-2966.2005.10039.x](https://doi.org/10.1111/j.1365-2966.2005.10039.x)
- [9] Chernyakova, M., Neronov, A., Aharonian F., et al.: 2009, *MNRAS*, 397, 2123 [doi:10.1111/j.1365-2966.2009.15116.x](https://doi.org/10.1111/j.1365-2966.2009.15116.x)
- [10] Johnston, S., Manchester, R.N., Lyne, A.G, et al.: 1992a, *ApJ*, 387, 37
- [11] Johnston, S., Lyne, A.G, Manchester, R.N., et al.: 1992b, *MNRAS*, 255, 401
- [12] Johnston, S., Manchester, R.N., Lyne, A.G, et al.: 1994, *MNRAS*, 268, 430
- [13] Johnston, S., Manchester, R.N., Lyne, A.G, et al.: 1996, *MNRAS*, 279, 1026
- [14] Johnston, S., Manchester, R.N., McConnell, D.: 1999, *MNRAS*, 302, 277
- [15] Johnston, S., Wex, N., Nicastro, L., et al.: 2001, *MNRAS*, 326, 643
- [16] Kaspi, V. M., Tavani M., Nagase F., et al.: 1995, *ApJ*, 453, 424 [doi:10.1086/176403](https://doi.org/10.1086/176403)
- [17] Khangulyan, D., Aharonian, F.A., Bogovalov, S.V., et al.: 2012, *ApJ*, 752, L17 [doi:10.1088/2041-8205/752/1/L17](https://doi.org/10.1088/2041-8205/752/1/L17)
- [18] Kong, S. W., Cheng, K. S., Huang, Y. F.: 2012, *ApJ*, 753, 127 [doi:10.1088/0004-637X/753/2/127](https://doi.org/10.1088/0004-637X/753/2/127)
- [19] Meintjes, P.J., van Soelen, B.: 2012, in *Multifrequency behaviour of high energy cosmic sources*, F. Giovannelli, L. Sabau-Graziati (eds.) *Mem. S.A.It.*, 83, 246
- [20] Moldón J., Johnston S., Ribó M., et al.: 2011, *ApJ*, 732, L10
- [21] Negueruela I., Ribó M., Herrero A., et al.: 2011, *ApJ*, 732, L11
- [22] Pavlov G. G., Chang C., Kargaltsev O.: 2011, *ApJ*, 730, 2
- [23] Schlickeiser, R.: 1985, *A&A*, 143, 431
- [24] Stawarz, L., Petrosian, V.: 2008, 681, 1725
- [25] Takata, J., Okazaki, A. T., Nagataki, S. et al.: 2012, *ApJ*, 750, 70
- [26] van Soelen, B., Meintjes, P.J.: 2011, *MNRAS*, 412, 1721
- [27] van Soelen, B., Meintjes, P.J., Odendaal, A., et al.: 2012, *MNRAS*, 426, 3135
- [28] Wang, N., Johnston, S., Manchester, R. N.: 2004, *MNRAS*, 351, 599

DISCUSSION

CARLOTTA PITTORI: In August 2010 AGILE reported the detection of gamma-ray activity above 100 MeV from the PSR B1259-63 region during the initial approach-to-periastron part of the orbit. Fermi did not confirm this detection, but later in November reported faint gamma-ray emission before the big 2011 flare. Are you aware of the Agile detection and can the model explain a ~ 100 MeV emission just before the disk passage?

BRIAN VAN SOELEN: Yes I am aware of the reported AGILE detection, as well as the Fermi follow-up analysis that did not detect emission. At this point I do not believe any model has completely accurately modelled the events that occurred around the previous periastron passage, including the reported detection by AGILE.